



ELSEVIER

Journal of Chromatography A, 967 (2002) 183–189

JOURNAL OF  
CHROMATOGRAPHY A

www.elsevier.com/locate/chroma

## Fiber optic multi-channel protein detector for use in preparative continuous annular chromatography

Athanasios Apostolidis<sup>a</sup>, Hartmut Lehmann<sup>b</sup>, Günter Schwotzer<sup>b</sup>, Reinhardt Willsch<sup>b</sup>,  
Albert Prior<sup>c</sup>, Jürgen Wolfgang<sup>c</sup>, Ingo Klimant<sup>a</sup>, Otto S. Wolfbeis<sup>a,\*</sup>

<sup>a</sup>University of Regensburg, Institute of Analytical Chemistry, Chemo- and Biosensors, D-93040 Regensburg, Germany

<sup>b</sup>Institute of Physical High Technology, Winzelaer Str. 10, D-07745 Jena, Germany

<sup>c</sup>Prior Separation Technology, Vorarlberger Wirtschaftspark, A-6840 Goetzis, Austria

Received 23 January 2002; received in revised form 4 June 2002; accepted 4 June 2002

### Abstract

Continuous annular chromatography is an effective method in the separation of preparative scale quantities of biological compounds including proteins where established batch chromatography borders on it. The need for identification or quantification of proteins triggered the development of respective detection units. Here, we describe two types of optical multi-channel detectors. The first is a fiber optic multi-channel detector suitable for the separation of aqueous protein solutions. The second is a technically improved (circular optic) device suitable for application in multi-channel detection. Specifically, UV-absorption measurements of proteins at 280 nm were carried out using newly designed fiber optic detectors having eight and 16 channels. Calibration plots were established for a series of stock solutions of known concentrations of proteins. Mathematical functions were derived from these calibration data to simulate the response of the detector. Limits of detection and the ranges of validity of the fit functions were determined. The 16-channel detector has a theoretical limit of detection that is equivalent to absorbance changes of  $10^{-4}$  units.

© 2002 Elsevier Science B.V. All rights reserved.

**Keywords:** Annular chromatography; Multi-channel optical detection; Fiber optics; Detection, LC; Preparative chromatography; Proteins

### 1. Introduction

One of the outcomes of modern biotechnology is the numerous proteins which can now be produced by yeast and other microbes in large quantities. The new production techniques require, however, new

methods for the separation and purification of the products of interest from the bulk material. Chromatography certainly is a most efficient method for the separation of biological compounds [1], but classical batch chromatography is not capable of processing the quantities of material that are turned over during industrial production.

Hence, numerous efforts were made to increase the capacity of chromatography columns by developing new methods [2,3]. Among those, annular chromatography (AC) [4–6] is particularly attractive and

\*Corresponding author. Tel.: +49-941-943-4065; fax: +49-941-943-4064.

E-mail address: [otto.wolfbeis@chemie.uni-regensburg.de](mailto:otto.wolfbeis@chemie.uni-regensburg.de) (O.S. Wolfbeis).

applicable to the separation of proteins [7–9]. AC enables continuous chromatography, with all components appearing simultaneously at different positions of the AC column. This method can largely increase the turnover and paves the way to preparative and even industrial scale manufacturing of proteins of high purity. A preparative-scale continuous annular chromatograph (P-CAC) for the separation of multi-component mixtures is commercially available and overcomes the limitations of batch chromatography in the isolation of proteins. Unfortunately, no adequate detectors have been described so far.

We have tackled this problem and designed a detection scheme for P-CAC that is intended for use mainly in protein chromatography. Depending on the application, several solutions for a detector are considered, but the need for non-invasive monitoring (for sterility reasons) led us to optical detection. Also, optical detection is established and has a wide range of applications in bioseparation. Optical detectors have the potential of being adjusted to a very specific and therefore rather selective wavelength, particularly in the visible part of the spectrum. Under the stipulations of wide applicability, wide dynamic range and technical simplicity, we considered UV-spectroscopic detection to be the method of choice.

However, a conventional detection cell (with each cell fitted with its own light source and light detector, respectively) was not taken into consideration for cost reasons and because of the expected opto-mechanical and opto-electronic complexity of the system. If applying fiber optics, two approaches appear to be possible. The first consists of sequential screening of the separated protein solutions using a rotating single detector unit. The second includes a series of independent detectors for each channel that are read simultaneously by opto-electronic hardware. The latter solution is deemed to be more appropriate for reasons of mechanical stability and the fact that it enables parallel on-line monitoring.

Thus, an optical scheme was preferred over other schemes due to its wider applicability (and potentially higher specificity) in bioseparation. The number of flow cells used in P-CAC (usually greater than 90) prevents the use of expensive single detectors. Fiber optics, in contrast, allow multi-site sampling even if using a single light source, provided fiber

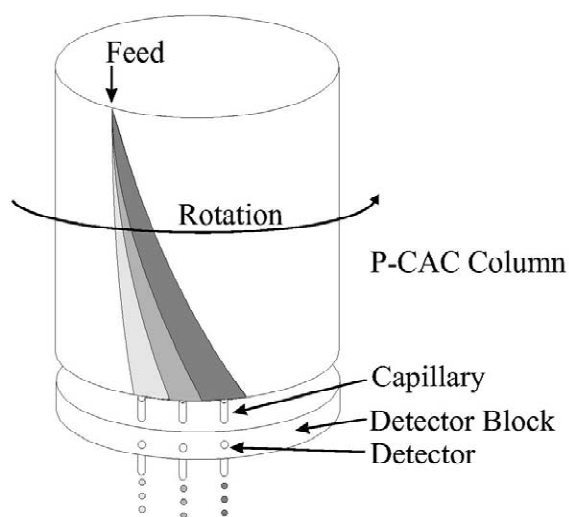


Fig. 1. Schematic view of the continuous annular chromatograph with the detector developed.

bundles are used [10]. In this work, we describe the first implementation of the resulting fiber optic detector array for P-CAC. As a first approach a fiber-optic eight-channel detector (FOD) was developed and characterised. A circular-optic 16-channel detector (COD) was developed to improve the performance of the device. Both designs are described in Section 3.

A schematic view of the arrangement and the working principle of the P-CAC and the detector is given in Fig. 1. The solution containing the protein to be purified is applied onto the column at one point, the so-called feed. Because of the rotation of the annulus, the fractions appear at different points at the bottom of the column and are guided through the capillaries of the detector block.

## 2. Experimental

### 2.1. Chemicals

All chemicals and proteins were of analytical grade and used without further purification. Disodium hydrogenphosphate ( $\text{Na}_2\text{HPO}_4 \cdot 12\text{H}_2\text{O}$ ), potassium dihydrogenphosphate ( $\text{KH}_2\text{PO}_4$ ), hemoglobin, L-tryptophane and L-tyrosine were purchased from Merck. Insulin,  $\alpha$ -chymotrypsin and cyto-

chrome *c* were from Serva (Heidelberg), lysozyme,  $\beta$ -lactoglobulin,  $\gamma$ -globulin and bovine serum albumin from Sigma (Munich).

## 2.2. Stock solutions

A 100 mM  $\text{Na}_2\text{HPO}_4/\text{KH}_2\text{PO}_4$  Sørensen buffer of pH 8 was prepared by dissolving 0.7483 g of  $\text{KH}_2\text{PO}_4$  and 16.8201 g of  $\text{Na}_2\text{HPO}_4 \cdot 12 \text{H}_2\text{O}$  in 100 ml of desalted water. Protein stock solutions were prepared by dissolving a weighed amount of protein in 100 ml of the buffer solution. In order to obtain standard solutions of lower concentration, defined volumes of the stock solution were diluted to 100 ml with buffer.

## 2.3. Measurements with the UV–Vis spectrometer

The absorption spectra of the amino acids (Tyr, Trp), proteins (BSA,  $\alpha$ -chymotrypsin, cytochrome *c*,  $\gamma$ -globulin, hemoglobin, insulin,  $\beta$ -lactoglobulin and lysozyme) and of vitamin  $\text{B}_{12}$  were acquired with a Perkin-Elmer Lambda 14 UV–Vis-spectrometer in the range from 200 to 600 nm. Quartz cuvettes ( $1 \times 1 \text{ cm}^2$ ) were used as absorption cells. Stock solutions with increasing concentration of the species of interest were examined. The maximum absorbance at the peak wavelength was determined and plotted against concentration. Aqueous protein solutions were also studied with the fiber optic eight-channel detector and the circular optic 16-channel UV-photometer to be described later (see Section 3).

## 2.4. Software

The software was developed on the National Instruments programming platform LabVIEW 4.0. It includes a chart recorder to display the present data acquired, and subroutines for data storage. The raw data are read out from the respective files and the dark signal (i.e. the thermal noise of the detector) from each channel is subtracted from the values measured to give the corrected intensity of the incident light. The corrected values at a given protein concentration were divided through the corrected blank values (buffer) to give the transmission of the solution. The refined data were then plotted and fit

functions were applied to determine the range of validity of the Lambert–Beer Law.

## 2.5. Experimental details

The light source was a xenon arc lamp from LEJ Jena (Germany) with a standard 280-nm bandpass filter (bandwidth 20 nm, in order to provide sufficient light intensity) from LOT-Oriel. The glass fiber bundle with a diameter of 1 cm was from Schott. The dimensions of the detector block are 16 cm in diameter and 2 cm in thickness. The quartz capillaries were 2.5 cm in diameter. Standard Si-photodiodes were used as detectors.

## 3. Results

### 3.1. The absorbance of proteins

Native proteins consist of a characteristic combination of 20 amino acids [1]. The average fraction of phenylalanine (Phe), tryptophane (Trp) and tyrosine (Tyr) in proteins is given in Table 1. The latter two show an absorbance peak at around 280–290 nm [11]. Therefore, the vast majority of proteins can be detected via their absorbance at this wavelength. The changes in the absorbance of selected proteins with increasing protein concentration in phosphate buffer of pH 8 are given in Table 2.

### 3.2. The eight-channel fiber optic detector (FOD) and the 16-channel circular optic detector (COD)

As a first prototype, a fiber optic eight-channel detector was developed. Based on the working principle of a single path UV-photometer, fiber optic waveguides were used to illuminate the flow cells. Optical fibers were also used to collect the trans-

Table 1  
Average fraction of aromatic amino acids in native proteins [11,12], and spectral data for aromatic amino acids

	%	$\varepsilon$ ( $\text{l mol}^{-1} \text{ cm}^{-1}$ )	$\lambda_{\text{max}}$ (nm)
Phenylalanine (Phe)	3.5	200	257
Tryptophane (Trp)	1.1	5600	280
Tyrosine (Tyr)	3.5	1400	274

Table 2

Initial slope ( $\Delta A/\text{mg protein}$ ) of the absorbance of aqueous protein solutions (phosphate buffer, pH 8.0) as measured with the fiber optic eight-channel UV photometer and limits of detection (LOD)

Protein	Initial slope ( $1 \text{ g}^{-1}$ )	LOD ( $\text{g l}^{-1}$ )	Linear range ( $\text{g l}^{-1}$ )
Bovine serum albumin	0.080	0.25	0–2.5
$\alpha$ -Chymotrypsin	0.245	0.08	0–2.0
Cytochrome <i>c</i>	0.304	0.07	0–4.3
$\gamma$ -Globulin	0.162	0.13	0–2.5
Hemoglobin	0.311	0.07	0–4.0
Insulin	0.131	0.16	0–1.0 <sup>a</sup>
$\beta$ -Lactoglobulin	0.126	0.16	0–3.2
Lysozyme	0.327	0.06	0–1.0

<sup>a</sup> Limited by solubility.

mitted light and guide it to a diode array used as detector. The transmitted light intensity was acquired (not shown here), and the respective absorbance calculated by a computer. The set-up of the FOD was validated with several target proteins.

After proving the feasibility of the method with the first prototype, a second one was developed to overcome the challenges of technical demands to the detector. Since the CAC column is of cylindrical shape, the detector also has to be adjusted to an annular shape so as to fit into one housing with the column. Fig. 2 shows a schematic view of the cross-section of the annular detector (COD), and Fig. 3 the top view of the device. The modular arrangement of

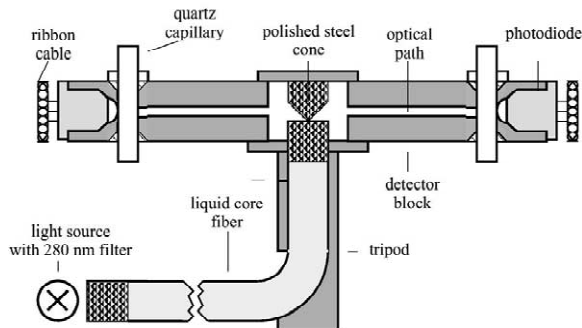


Fig. 2. Schematic view of the cross-section of the circular fiber optic 16-channel detector (COD). The liquid core fiber optic guides 280-nm light to a polished steel cone which reflects light into the drilled holes ("optical path") of the detector block. After passing the quartz capillary containing the flowing sample, transmitted light is detected by the photodiode. The ribbon cable links the photodiodes to the calculator. For a top view see Fig. 2.

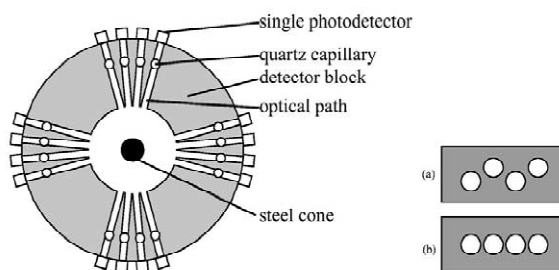


Fig. 3. Left: Top view of the circular fiber optic detector device. Light from the external light source (Fig. 1) hits the steel cone and is coupled into the optical path drilled into the detector block. The quartz capillaries containing protein solution are placed vertically to the optical path. A single photodetector is placed at the end of each optical path. Right: (a) zig-zag arrangement of optical paths; (b) plain arrangement of optical paths.

the components is a major advantage in terms of the applicability of the COD. The use of a single light source can keep the costs low since this part represents a major cost factor. Positioning of the optical filters in front of the light source outside the detection unit facilitates the replacement of damaged filters and a change in the detection wavelength. No dismantling of the P-CAC is necessary. To provide a continuous flow, quartz capillaries are used as flow-through cells. The need for the possibility of changing components is also governed by the need to maintain sterility inside the detection cell. The photodiodes (Si-photodiodes) used are inexpensive. In fact, they are often used for monitoring burners as used for heating. All these facets make the COD affordable and, hence, suitable for practical application.

### 3.3. Detection of proteins with the COD

The dark current from each detector photodiode was determined first. The resulting data were used to correct the transmission values of the calibration fluid by subtraction of the dark current. The performance of the COD was checked by measurements of aqueous solutions of Tyr and Trp as reference. Then, hemoglobin, cytochrome *c*, lysozyme and BSA were characterised. The calibration plot for hemoglobin is given in Fig. 4. Respective plots were also obtained for cytochrome *c*, lysozyme and BSA which can be described by a function  $A=k[\text{protein}]$ ,

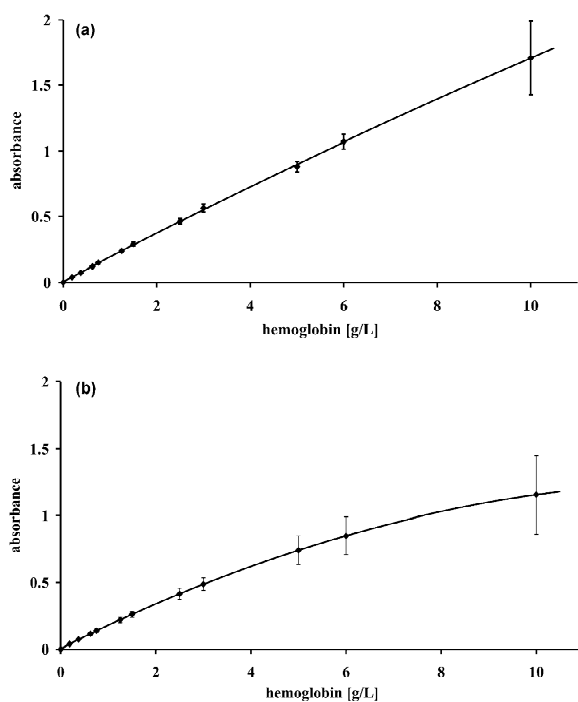


Fig. 4. Calibration plots of aqueous hemoglobin solutions in phosphate buffer of pH 8 acquired with the COD schematically shown in Fig. 2. The plot in (a) has a  $k$  of  $0.175 \text{ l g}^{-1}$ . The light guiding channels (“optical paths”) had a diameter of 2.5 mm. The plot in (b) has a  $k$  of  $0.131 \text{ l g}^{-1}$ . The light guiding channels (“optical paths”) had a diameter of 2.0 mm. Both plots were obtained independent of whether arrangements (a) or (b) (Fig. 2) were used.

$k$  being 0.088, 0.109 and  $0.027 \text{ l g}^{-1}$ , respectively, if an optical path diameter of 2.5 mm is employed. The channel to channel reproducibility was better than 10%. The limits of detection (LOD) were calculated from the calibration plots of the proteins. The LODs were calculated for a noise level of 0.006 AU and assuming an  $S/N$  ratio of 3:1, and are given in Table 2.

Most proteins show, however, a downward deviation from linearity in their calibration plots as seen for hemoglobin in Fig. 4(b). A reason for this observation is the round shape of the flow cells: The refractive index of the solution changes with rising protein concentration. Hence, light not only passes the cell but partially is guided through the glass walls of the cell, thereby circumventing the protein solution. This effect becomes increasingly efficient with

the increase in the refractive index of the aqueous solution and leads to reduction of the absorbance of the sample solution.

### 3.4. Long-term stability and linearity of the COD

The long-term stability of the 16-channel circular optic detector (COD) was also investigated. First, the absorbance of plain buffer solution that was pumped through the flow cells was monitored over several hours. A baseline drift of only  $\pm 0.001 \text{ AU per h}$  was found for the COD (provided the temperature was kept constant). Next, various proteins were characterised in terms of the linearity of their response. Figs. 4 and 5 show the calibration plots for hemoglobin and cytochrome *c*. The plots on the upper panel (a) were obtained with optical paths of 2.5 mm,

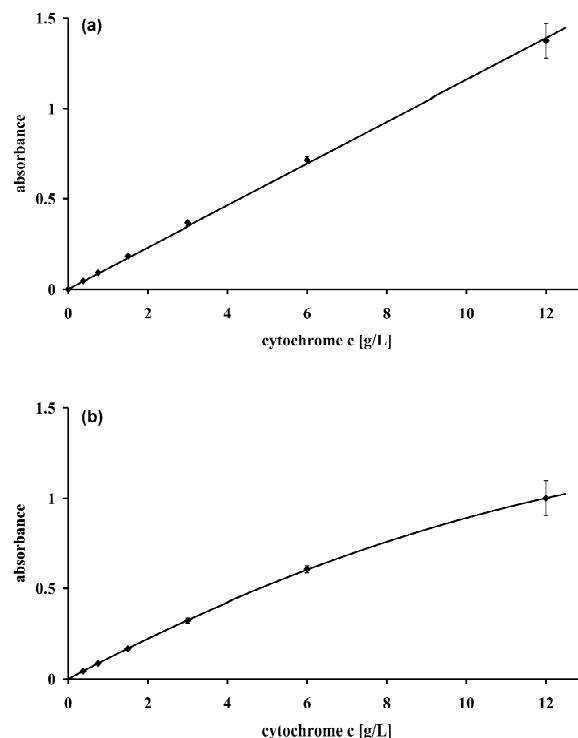


Fig. 5. Calibration plots of aqueous cytochrome *c* solutions in phosphate buffer at pH 8. The plot in (a) has a  $k$  of  $0.116 \text{ l g}^{-1}$ . The light guiding channels (“optical paths”) had a diameter of 2.5 mm. The plot in (b) has a  $k$  of  $0.088 \text{ l g}^{-1}$ . The light guiding channels (“optical paths”) had a diameter of 2.0 mm. Both plots were obtained independent of whether arrangements (a) or (b) (Fig. 2) were used.

while the plots on the lower panel (b) were obtained with 2-mm optical paths. They can be described with a linear fit function in the concentration range from 0 to at least  $5 \text{ l g}^{-1}$  protein. Negative deviations from the Lambert–Beer Law can be explained, again by the quality of the optical filters used. At bandwidths of approximately 20 nm, it is reasonable that for colored proteins with additional absorbance peaks at higher wavelengths and to a higher degree for non-coloured proteins, light is transmitted without interacting with the sample. This error in monochromaticity of the incident light causes a negative deviation of the calibration plot with rising protein concentration.

### 3.5. Position effects

The photodetectors were combined to four different groups of four detectors each in order to determine the effect of the position of the measuring

channel relative to the centre of the light field as well as the diameter of the optical path. The first group of detectors is assigned to a zig-zag arrangement of the optical paths (Fig. 3a) and a length of 2.5 mm for the optical path. The second group has a linear arrangement (Fig. 3b) and a path length of 2.5 mm. The third group has a zig-zag arrangement and a 2-mm path, and the fourth group a linear arrangement and a 2-mm path, respectively. As shown in Figs. 4 and 5, the arrangement of the optical path as either zig-zag or linear has no major effect on the response of the detector. An arrangement of 90 channels within a P-CAC plant is therefore considered to be possible. This is an important feature for the application of the detection system in the P-CAC where space is limited by the radius of the annulus containing the separation media. Another obvious result is that each channel has to be calibrated separately, at least once. The reproducibility of the signals is very good as shown in Fig. 6. The standard deviation of the response was determined to be lower than 1%.

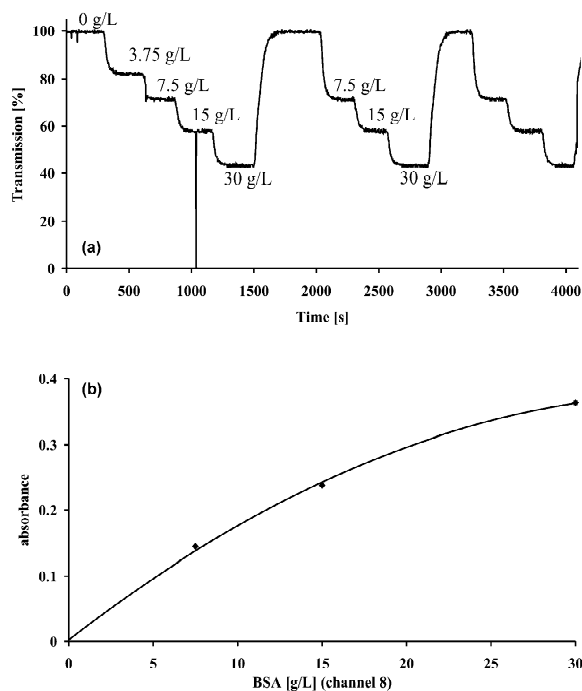


Fig. 6. Reproducibility of the absorbance within a single channel. (a) Time drive of the absorbance of aqueous BSA solutions in channel 8. (b) Calibration plot (including error bars) of aqueous BSA solutions in phosphate buffer of pH 8 calculated for the data from one channel.

## 4. Discussion

Depending on the application, several configurations for a detector are conceivable, but the need for: (1) versatility, (2) wide applicability, (3) large dynamic range, (4) solid-state monitoring, along with the feature of highly parallel detection if fiber optics are used, led to an optical detection scheme. For high protein concentrations, refractive index detection may be another (but in terms of sensitivity less favourable) parameter, while fluorescence may be the method of choice provided that proteins are studied that contain Tyr or Trp. By making use of a fiber optic primary (liquid core) light guide, the COD is comparably simple in terms of opto-mechanics and opto-electronics. The results show that all proteins studied were detectable by the circular optic UV detector (COD) over the concentration range encountered in practice. Scaling up the number of detection channels to 90 has been accomplished meanwhile. The COD presented here may even be spectrally modified by adding filters (or a filter wheel) with a transmittance specific for any component of interest (e.g. proteins, precious metals). By applying two-wavelength measurements, internal

referencing becomes possible [13–15] and thus may further enhance the performance of the system.

## References

- [1] D. Voet, J.G. Voet, *Biochemistry*, Wiley, New York, 1995, p. 72.
- [2] M.V. Sussman, R.N.S. Rathore, *Chromatographia* 8 (1975) 55.
- [3] K. Reissner, A. Prior, J. Wolfgang, H.J. Bart, C.H. Byers, *J. Chromatogr. A* 763 (1997) 49.
- [4] A.J.P. Martin, *Discuss. Faraday Soc.* 7 (1949) 332.
- [5] W. Grassman, K. Hannig, *Angew. Chem.* 62 (1950) 170.
- [6] C.D. Scott, R.D. Spence, W. Sisson, *J. Chromatogr.* 126 (1976) 381.
- [7] G.F. Bloomingburg, J.S. Bauer, G. Carta, C.H. Byers, *Ind. Eng. Chem. Res.* 30 (1991) 1061.
- [8] G.F. Bloomingburg, G. Carta, *Chem. Eng. J.* 55 (1994) B19.
- [9] K. Reissner, A. Prior, J. Wolfgang, H.J. Bart, C.H. Byers, *J. Chromatogr. A* 763 (1997) 49.
- [10] O.S. Wolfbeis (Ed.), *Fiber Optic Chemical Sensors and Biosensors*, CRC Press, Boca Raton, FL, 1991.
- [11] M.H. Klapper, *Biochem. Biophys. Res. Commun.* 78 (1977) 1020.
- [12] F.X. Schmid, in: T.E. Creighton (Ed.), *Protein Structure—A Practical Approach*, IRL Press, Oxford, 1989.
- [13] J. Floch, S. Blain, D. Birot, P. Treguer, *Anal. Chim. Acta* 377 (2-3) (1998) 157.
- [14] E.A.G. Zagatto, M.A.Z. Arruda, A.O. Jacintho, I.L. Mattos, *Anal. Chim. Acta* 234 (1990) 153.
- [15] A. Daniel, D. Birot, M. Lehaitre, J. Poncin, *Anal. Chim. Acta* 308 (1995) 413.